AN IMAGING LIDAR FOR MONITORING OF OIL SPILL AND UV FLUORESCENT SUBSTANCES AT THE WATER SURFACE AND SUBSURFACE

Masahiko Sasano[(1)], Kazuo Hitomi[(1)], Hiroshi Yamanouchi[(1)] and Susumu Yamagishi[(2)]

[(1)] *Navigation and System Engineering Department, National Maritime Research Institute*
Shinkawa 6-38-1 Mitaka Tokyo 181-0004 Japan, sasano@nmri.go.jp
[(2)] *Collaboration Center, Tokyo University of Marine Science and Technology*
Konan 4-5-7 Minato-ku Tokyo 108-8477 Japan, syamagi@e.kaiyodai.ac.jp

ABSTRACT

We developed an imaging lidar for monitoring oil spills and other UV fluorescent substances on the ocean. The lidar consists of a 355 nm UV pulsed Nd:YAG laser, four optical lenses with respective optical filters, and a gated ICCD camera. The 2-D images of oil film were successfully observed in the daytime as laser-induced fluorescence patterns using a helicopter-based lidar system. Additionally, we also succeeded in detecting fluorescence from a sheet of paper, a UV fluorescent substance, at the bottom of a 34 m depth basin.

1. INTRODUCTION

Lidar is a powerful tool for detecting pollutants such as oil spills on the ocean [1]. It is possible to detect oil spills in the day and at night by observing the laser-induced fluorescence from the ocean surface, and it is also possible to distinguish oil spills precisely from other substances by laser-induced spectroscopy. Since this method is non-contact sensing, airborne observation is available with high-speed movement.

In order to monitor a large ocean area, in addition to a high speed platform, it is also important to maintain a wide swath. There are two methods of achieving this requirement; the scanning method and the imaging method.

The scanning method observes one direction in one shot, and scans the observation direction over time. It has a high signal-to-noise ratio and high time resolution in one direction. The scanning method creates a time-gap between each shot, which makes the platform stability important. On the other hand, the imaging method is a method of observing a wide solid angle in one shot. The spread laser beam makes less lidar return signal in one direction, and the 2-D photo-sensor has comparatively less time resolution. But it has high angular resolution, and it is comparatively easy to make a 2-D image of the target.

Several lidar systems have been developed to monitor oil spills, most of which are the airplane-based scanning type or vertical observation type [2]-[4]. In this study, we considered not only the airplane platform but also the helicopter or ship platform, which is unstable and sometimes moves at low speed. Therefore, we developed an imaging lidar to monitor oil spills and massive chemical pollutants on the ocean [5][6]. This system records an image of UV fluorescent substances on the water surface and subsurface, and the observed image does not need to be corrected for platform attitude or moving speed for interpretation. In addition, it facilitates the recognition of the target by the operator.

2. SYSTEM

The schematics of the helicopter-based fluorescence imaging lidar for oil spill monitoring are shown in Fig.1. The specifications of the system are shown in Table.1. The transmittance laser is Nd:YAG with third harmonic generator (wavelength 355 nm), and the energy is 50 mJ/pulse with 8 Hz repetition. The laser direction is toward the nadir and the beam divergence is adjustable from 1 mrad to 100 mrad depending on the situation. Since the helicopter flies between 150 m and 300 m in height, the laser footprint on the sea surface has a diameter between 0.15 m and 30 m, and the lidar signal from the sea surface occurs approximately 1 to 2 micro seconds after the laser emission.

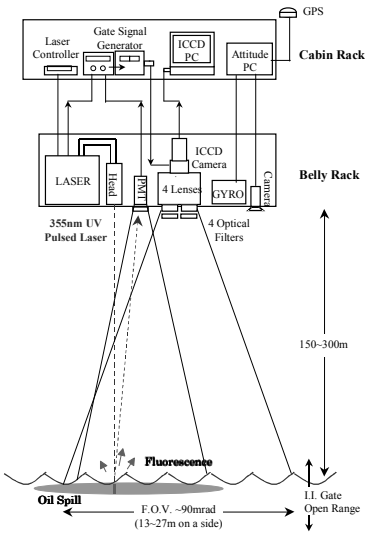

Fig.1 Schematic diagram of the helicopter-based fluorescence imaging lidar for oil spill monitoring.

Table.1 Specifications of the helicopter-based fluorescence imaging lidar.

Laser	Type	Nd:YAG(THG)
	Wavelength	355nm
	Energy	50mJ/pulse
	Repetition	8Hz (Max 10Hz)
	Beam Divergence	1 – 100 mrad
Optical filter & Lens	Peak wavelength	405, 436, 442, 486nm
	FWHM	10nm
	Lens diameter	5cm
ICCD camera (Image Intensifier + CCD camera)	I.I. Gain	$7 * 10^4$
	CCD camera Pixel Size	1024 * 1024 (512*512 / lens)
	Digitizing	12bit
	F.O.V.	90mrad
	Recording Repetition	8Hz
GPS	Position Resolution	0.9m horizontal 1.6m vertical
Attitude Measurement Equipment	Attitude Resolution	0.2deg

The receiver consists of an ICCD camera and four optical lenses. The focal plane of the image intensifier is divided into four parts, and each part is used as a focal plane of each optical lens that is 5 cm in diameter. Four images have 90 mrad by 90 mrad field of view, and an independent wavelength band of 405.0, 435.8, 441.6 and 486.1 nm respectively. This design achieves an observation of four optical images at respective wavelength bands in exactly same timing.

The pixel size of the CCD camera is 1024 by 1024, and therefore one image with one wavelength band corresponds to 512 by 512 pixels, and each pixel has 12 bits of ADC resolution.

The exposure time of the ICCD camera is gated to 200 ns including the timing of the lidar signal from the ocean surface, so that the background light from the ocean surface is reduced and the signal-to-noise ratio of the fluorescence image is enhanced. To realize this gate function, the laser traveling time between the helicopter and the ocean surface needs to be preset in the system, but the distance along with the laser track always changes with the helicopter attitude and position. Therefore, there is a special circuit to preset the ICCD gate timing every laser shot using the previous lidar signal timing. Meanwhile, the attitude and position of the helicopter are recorded by the attitude meter and the GPS. Those data are used for the correction of lidar observation direction and distance.

3. SURFACE DETECTION

An international offshore experiment on oil spill monitoring and control, “DEPOL04” has been conducted off the coast of France in May 2004. The helicopter-based fluorescence lidar observation has been held during the experiment. Fig.2 shows the four observed images by one shot of “narrow beam”, a laser beam with 1 mrad of divergence, from 150 m height to the target of seawater in the daytime. The intense spot of the lidar signal is shown in the image of 405 nm out of four images, which is the wavelength in which water Raman emission is dominant [7].

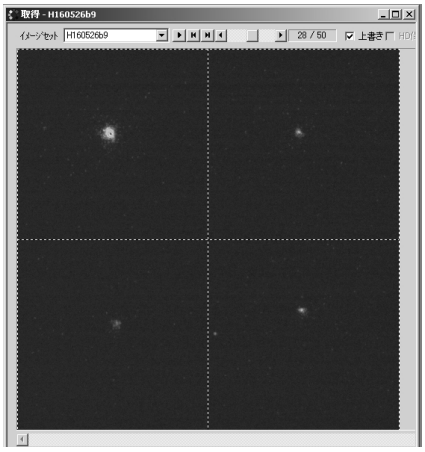

Fig.2 UV laser induced images of sea water (narrow beam). The wavelengths are 405, 436, 442, 486nm respectively, counter-clockwise from the top-left.

In addition, the helicopter-based lidar experiments of oil film detection have been held inside an airport in Japan in January and March 2005. Three portable pools were built with one diesel oil film, one kerosene film and the other empty. The average thickness of oil layers was around 5 mm. In January, the laser was set to narrow beam with a divergence of 1 mrad, shot the oil film from the helicopter, and observed the laser-induced fluorescence from the oil film. Views of the experiments are shown in Fig.3.

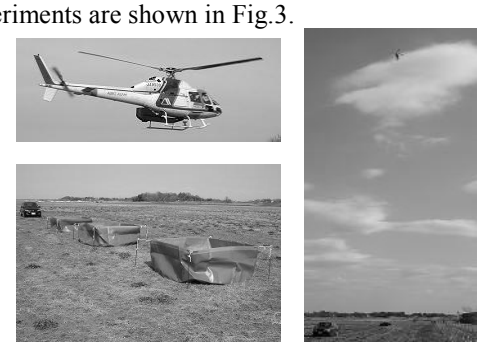

Fig.3 Views of the helicopter-based fluorescence lidar observation with the target of three portable pools.

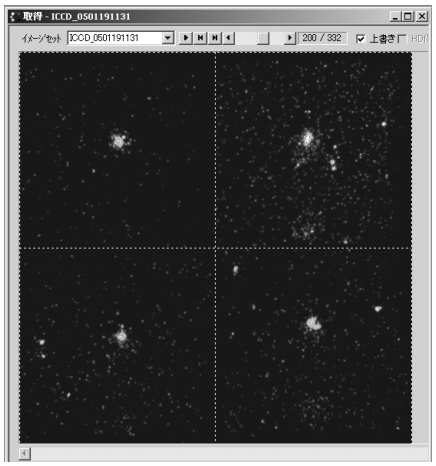

Fig.4 UV laser induced images of the diesel oil film in the portable pool (narrow beam).

Fig.4 shows the four observed images by one shot from 150 m height to the target of the thin diesel oil film in the daytime. Intense spots of lidar signal are shown in all images, and this is a typical characteristic of the laser-induced oil fluorescence; strong emission and broad spectrum.

In March, the laser was set to “wide beam”, the laser beam with approximately 60 mrad of divergence, shot the oil film from the helicopter, and observed the 2-D images of laser-induced fluorescence. Fig.5 shows the four observed images by one shot from 140 m height to the target of portable pools with a 5 mm thick diesel oil film in the daytime. As in the case of the narrow beam, all four images show the fluorescence from the oil film, and the 2-D intensity distributions show the oil film area.

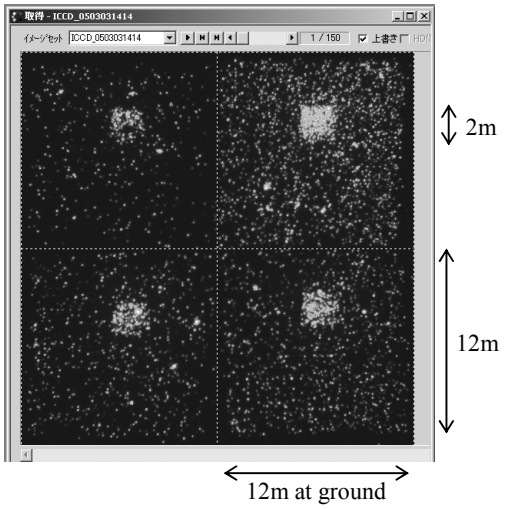

Fig.5 UV laser induced images of the diesel oil film in the portable pool (wide beam).

4. SUBSURFACE DETECTION

In August 2003, in order to test the detection capability of fluorescence lidar to the UV fluorescent substance in the water, lidar observation has been conducted at the 34 m depth basin in NMRI. The target, a sheet of paper as an example of UV fluorescent substance, was set in the bottom of the basin. The fluorescence lidar system was set at 5 m height from the water surface, and fixed the observation direction with the laser incident angle of 8 degrees. The 34 m depth basin was filled by filtered clear well water, and the water surface was static. Because all the basin was in the building, background light was at the nighttime level. Fig.6 shows the schematics of the UV laser-induced subsurface emission experiment, and Fig.7 shows the four observed images by one shot of narrow beam with a divergence of 1 mrad.

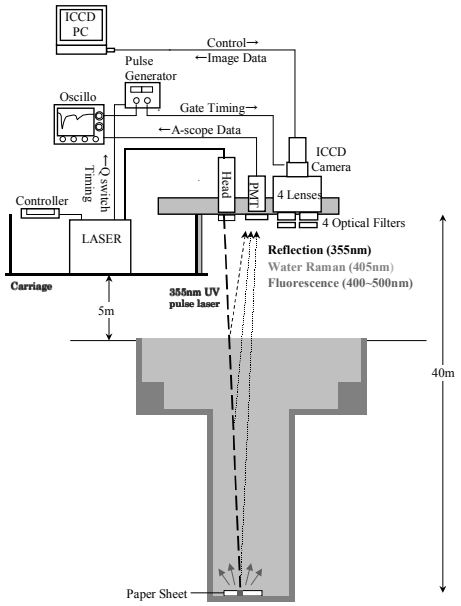

Fig.6 Schematic diagram of the UV laser-induced subsurface emission experiment at the 34m depth basin.

The intense spots of fluorescence from the paper sheet are shown in all of the three images except the 405 nm image. In the 405 nm image, strong water Raman emission is shown along with the laser track in the water. The distances from the emission points on the image data to the ICCD camera are computable using the geometrical position of the laser, the ICCD camera and the water surface. Fig.8 shows the Y-direction averaged intensity of the 405 nm image. Additionally, the expected curve from water Raman emission is shown in the same figure. This calculation is excluding the laser divergence and multiple scattering effect, and assumed that the water attenuation coefficient was

clearest natural water level [8]. The observed curve of lidar signal is mostly comparable to the expected curve, but the difference becomes significant with depth. This lidar signal excess implies the multiple scattering effect, and the small plateau at near the center of X-axis is thought to be fluorescence from the paper sheet.

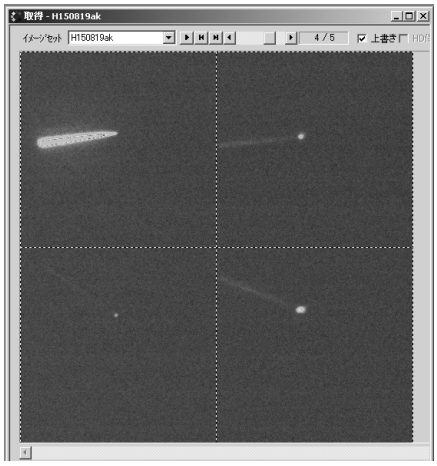

Fig.7 UV laser induced images of water Raman emission and fluorescence from the paper sheet at the 34m depth basin (narrow beam).

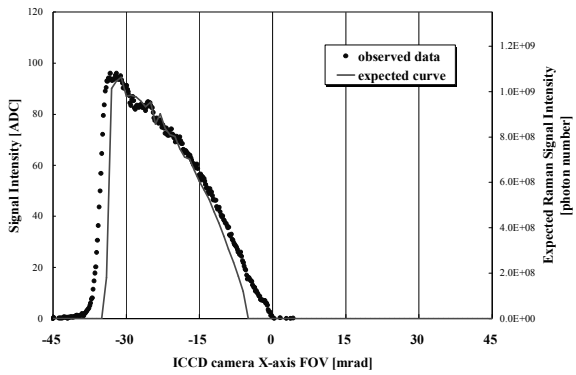

Fig.8 The observed intensity distribution of Y-direction averaged 405nm image, and the expected water Raman emission intensity curve.

5. CONCLUSIONS

We developed UV fluorescence imaging lidar, and succeeded in the detecting and distinguishing oil films from seawater by helicopter experiments in the daytime. The 2-D oil film images were obtained by this system with wide laser beam. These results lead that the helicopter-based imaging lidar is a powerful tool for monitoring oil spill and for searching the runoff source day and night.

Meanwhile, we confirmed the detection capability of our system for subsurface UV fluorescent substances using 34 m depth basin. It shows the potential of our system for finding underwater oils and fluorescent objects such as sunken ships.

ACKNOWLEDGEMENTS

This study was sponsored by the fund for global environmental protection, Ministry of the Environment, Japan. We also express our appreciation the support of CEDRE, France in the experiment “DEPOL04”.

REFERENCES

1. Brown C.E. and Fingas M.F., Review of the development of laser fluorosensors for oil spill application, *Marine Pollution Bulletin* Vol.47 (2003) 477-484.

2. Brown C.E., Marois R. and Fingas M.F., Airborne Oil Spill Sensor Testing: Progress and Recent Developments, *Proc. of Int. Oil Spill Conf. 2001* (2001) 917-921.

3. Hengstermann T. and Reuter R., Lidar fluorosensing of mineral oil spills on the sea surface, *Applied Optics* Vol.29 (1990) 3218-3227.

4. Lennon M., Babichenko S. and Mercier G., Operational quantitative mapping of oil pollutions at sea by joint use of an Hyperspectral Imager and a Fluorescence Lidar System on-board a fixed wing aircraft, *Proc. of the EARSEL*, Vol.5, No.1 (2006).

5. Yamagishi S., Hitomi K., Yamanouchi H., Yamaguchi Y. and Shibata T., Hyperspectral Remote Sensing of the Ocean, *SPIE* Vol.4154 (2000) 136-144

6. Sasano M., Hitomi K., Yamanouchi H., Taguchi N. and Yamagishi S., Remote Sensing of Oil Spill using a Helicopter-based Fluorescence Imaging LIDAR, *Proc. of 4th World Congress on Industrial Process Tomography* Vol.1 (2005) 58-63.

7. Bristow M., Nielsen D., Bundy D. and Furtek R., Use of water Raman emission to correct airborne laser fluorosensor data for effects of water optical attenuation, *Applied Optics* Vol.20 (1981) 2889-2906

8. Raymond C. S. and Karen S. B., Optical properties of the clearest natural waters (200-800nm), *Applied Optics* Vol.20 (1981) 177-184.